ACS APPLIED MATERIALS & INTERFACES

Research Article

www.acsami.org

Fluorescent Porous Film Modified Polymer Optical Fiber via "Click" Chemistry: Stable Dye Dispersion and Trace Explosive Detection

Jiajun Ma, Ling Lv, Gang Zou, and Qijin Zhang*

CAS Key Laboratory of Soft Matter Chemistry, Collaborative Innovation Center of Chemistry for Energy Materials, Department of Polymer Science and Engineering, Anhui Key Laboratory of Optoelectronic Science and Technology, University of Science and Technology of China, Hefei, Anhui 230026, China

Supporting Information

ABSTRACT: In this paper, we report a facile strategy to fabricate fluorescent porous thin film on the surface of U-bent poly(methyl methacrylate) optical fiber (U-bent POF) *in situ* via "click" polymerization for vapor phase sensing of explosives. Upon irradiation of evanescent UV light transmitting within the fiber under ambient condition, a porous film (POSS-thiol cross-linking film, PTCF) is synthesized on the side surface of the fiber by a thiol−ene "click" reaction of vinyl-functionalized polyhedral oligomeric silsesquioxanes (POSS-V8) and alkane dithiols. When vinyl-functionalized porphyrin, containing four allyl substituents at the periphery, is added into precursors for the polymerization, fluorescence porphyrin can be covalently bonded into the cross-linked network of PTCF. This "fastened" way reduces the aggregation-induced fluorescence self-quenching of porphyrin and enhances the physicochemical stability of the porous film on the surface of U-bent POF. Fluorescent signals of the PTCF/U-bent POF probe made by this method exhibit high fluorescence quenching toward trace TNT and DNT vapor and the highest fluorescence quenching efficiency is observed for 1, 6-hexanedimercaptan-based film. In addition, because of the presence of POSS-V8 with multi cross-linkable groups, PTCF exhibits well-organized pore network and stable dye dispersion, which not only causes fast and sensitive fluorescence quenching against vapors of nitroaromatic compounds, but also provides a repeatability of the probing performance.

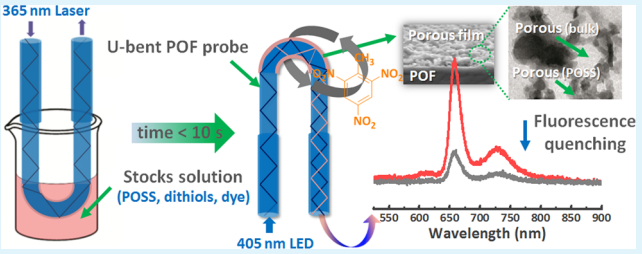

KEYWORDS: *poly(methyl methacrylate) optical fiber, explosive detection, porous film, fluorescent quenching, click chemistry*

INTRODUCTION

Rapid and accurate detection of explosives, including 2,4,6-trinitrotoluene (TNT) and 2,4-dinitrotoluene (DNT), has become increasingly important in the past few years because of homeland security, environmental protection and industrial safety control.[1−3] Various methods have been developed for nitro-explosives detection, such as desorption electrospray ionization mass spectrometry (DESI-MS),[4] gas chromatography and mass spectrometry (GC-MS),[5] surface-enhanced Raman spectroscopy (SERS),[6] and ion mobility spectrometry.[7] However, the expensive and complicated manipulation is the bottleneck for popularization of these technologies. Sensor system requirements consist of cost-effective, fine and reliable measurements. Fluorescent materials for development of sensitive explosive detection have the advantage of both human visual processing ability and instrumental evaluation.[8−12] The solution system containing fluorescent dye is more suitable to use on monitoring an aquatic environment.[13] Dyes based on a fluorescence quenching mechanism can be conveniently utilized to fabricate optical devices in order to collect data from a remote location.[14,15] Among these devices, optical fiber sensor offers many advantages, such as lower cost, greater portability, and the feasibility of creating sensor networks.

Poly(methyl methacrylate) optical fibers (POF) are usually chosen to build platforms as their large core, ease of handling and connections, flexibility, visible wavelength operating range, high numerical aperture and low cost test equipment.[16−18] These characteristics make them attractive for a number of applications in gratings fabrication,[19] optical amplification,[18] random fiber laser,[20] and chemical or biological sensors.[21] On the other hand, it is already known that monitoring of evanescent wave (absorption or fluorescence characteristics) in inorganic silica waveguides is often preferred for measuring oxygen,[22] ammonia,[23] pH,[24] temperature,[25] and explosives vapor.[26−28] Porous structure, which is always prepared by the mild sol−gel process,[29−31] is very critical for fiber-optic evanescent wave sensor[22−24] and other devices[32−34] because of the easy permeation capacity of analytes into the responsive layer. Sensitive dyes used for the preparation of optical fiber sensors can be immobilized in the homogeneous porous layer through adsorption or entrapment.[22,23,33] However, in any case, the nature of organic compounds causes a scarce compatibility with the inorganic silica matrix, leading to leaching out of the

Received: September 2, 2014
Accepted: December 9, 2014
Published: December 9, 2014

dx.doi.org/10.1021/am505950c | ACS Appl. Mater. Interfaces 2015, 7, 241−249

sensitive species from the support and aggregation-induced fluorescence self-quenching of dyes. One effective way to overcome this problem is to create covalent bonding or effective interactions between the dyes and the embedding matrix.[8,35] Further, ruggedness of the surface is also an important requirement for the fiber sensor to be used in this field. If the approach described above for the preparation of inorganic silica waveguides is applied to fabrication of a POF probe, an ineffective interaction between the organic poly(methyl methacrylate) and the inorganic component would be found, resulting in an unstable device with physical discontinuity between the optical fiber and the sensitive film.

Hybrid organic−inorganic porous materials[36−38] is an ideal choice to improve the compatibility for a POF sensor. In fact, when the organic part of the hybrids inside the sensor materials has a polymeric nature, it can play multiple roles: it can improve the adhesion between the polymer substrate and the whole sensitive hybrids by the hydrophobic interaction;[38−40] its chemical structure allows the tuning of the kinetic response of the sensor by controlling the diffusion rate of the vapor analyte inside the porous matrix and its interaction with the sensitive dyes; its organic nature can allow better chemical interactions with the organic indicators dispersed in the hybrid matrix.

In view of the analysis above, in this work, a new strategy is proposed to achieve these characteristics for a POF probe by fabrication of hybrid organic−inorganic fluorescent porous thin film (POSS-thiol cross-linking film, PTCF) modified U-bent POF *in situ* via "click" polymerization. The precursors, vinyl-functionalized polyhedral oligomeric silsesquioxanes (POSS-V8), allyl-functionalized porphyrin and alkane dithiols, can rapidly react upon irradiation of evanescent UV light transmitting within POF under ambient condition. The interest of this route is to provide a simple method to implement sensitive porous films on a surface of POF. The fiber probe obtained in this way may have two characters. One is that fluorescent molecule with active substituents can be covalently bonded into the network, and the second is that the pore-size distribution of thin film can be easily adjusted by using alkane dithiols with different chain length. Therefore, the work reported here is concentrated on investigation on the reproducible fabrication of U-bent POF probe containing porphyrin as sensitive dye and the vapor phase detection of explosives by this fiber probe.

EXPERIMENTAL SECTION

Materials and Characterization. Vinyl-functionalized polyhedral oligomeric silsesquioxanes (POSS-V8) (Hybrid Plastics Inc., USA), 1,6-hexanedimercaptan was synthesized according to literature,[41] 2, 2-dimethoxy-2-phenyl-acetophenone (DMPA) (99%, Sigma-Aldrich), allyl bromide (AR, 98%, Energy Chemical, China), benzoin dimethyl ether, and 4-hydroxybenzaldehyde (AR, 98%, Aladdin Industrial Corporation, China) were used without further purification. Anhydrous potassium carbonate (CP, 99.5%, Sinopharm Chemical Reagent Co., Ltd.) was used as received. Pyrrole, acetone, propionic acid and tetrahydrofuran (THF) (CP, 98%, Sinopharm Chemical Reagent Co., Ltd.) were purified by standard method. Other solvents purchased from Sinopharm Chemical Reagent Co., Ltd. were used without further purification. Thiol-teminated polyethylene glycol (SH-PEG-SH, M_n = 600, 1000, and 2000 Da) was synthesized according to literature.[42] Tetrakis(4-carboxyphenyl)porphyrin (TCPP) was synthesized according to literature.[43]

Transmission electron microscopy (TEM) bright-field images were taken using a FEI Tecnai G2 F30 microscope operated at 200 kV. TEM samples were carried out by cutting off sensory section from U-bent POF probe and dissolved in acetone and then filtrated. The obtained solid was dispersed in ethanol by ultrasonic. A drop of the suspension was placed on a holey carbon-coated copper grid. ^{1}H NMR spectra were recorded at ambient temperature with a Bruker AMX300 spectrometer. Scanning electron microscopy (SEM) images were taken with FEI Quanta 200F ESEM microscope at low vacuum conditions. MALDI-TOF mass analysis was performed on a Voyager-De STR instrument. Fourier transform infrared spectra (FTIR) were recorded on a Nicolet Nexus 470 IR spectrometer as KBr pellets. The nitrogen-sorption experiments were performed at 77 K on a Quannitrogen-sorption experiments. Thermogravimetric analysis (TGA) was performed on a TA SDT Q600 simultaneous DTA-TGA at a heating rate of 20 °C min^{-1}. UV−vis absorption and transmission spectra were recorded by Shimadzu UV2550 spectrophotometer. Fluorescence spectra were recorded by Shimadzu RF5301PC spectrophotometer. A contact angle meter (OCA 30, Dataphysics) was used to measure the static water contact angles on PTCF (dip-coated of the suspension onto the surface of the quartz plate). Water droplets of 0.4 μL volume were utilized and Laplace−Young fitting was applied on contact angle measurements.

Synthesis of 4-(Allyloxy)benzaldehyde. To the solution of 4-hydroxybenzaldehyde (16.1 g, 0.13 mol) in acetone (60 mL) was added K_2CO_3 (19 g, 0.14 mol) at room temperature under N_2. Allyl bromide (11.9 mL, 0.14 mol) was added at room temperature and the mixture was stirred for 2 h. The reaction mixture was then heated to reflux and stirred for another 3 h. After being cooled to room temperature, the mixture was filtered and washed with acetone, and then the solvent was evaporated. Purification by flash chromatography (hexane:ethyl acetate = 5:1, V/V, R_f = 0.46) afforded 4-(allyloxy)-benzaldehyde (73.4%, 15.7 g) as a colorless oil. ^{1}H NMR ($CDCl_3$, 400 MHz): δ 9.88 (s, 1H), 7.82 (d, 2H), 7.01 (d, 2H), 6.04 (dddd, 1H), 5.43 (dd, 1H), 5.32 (dd, 1H), 4.64−4.58 (m, 2H). Good correspondence was found in the literature.[44]

Synthesis of meso-Tetrakis[4-(allyloxy)phenyllporphrin (Allylporphyrin). 4-(Allyloxy)benzaldehyde (10.7 g, 0.066 mol) in butyric acid (100 mL) was brought to reflux under nitrogen. Pyrrole (4.4 g, 0.066 mol) was then added and reflux continued for 3 h. The reaction mixture was allowed to cool to room temperature and kept overnight in a refrigerator. The solid was filtered, washed with hot water to remove traces of butyric acid, and dried at 60 °C in a vacuum oven. Further Purification by column chromatography over silica gel (dichloromethane, R_f = 0.34) afforded a violet crystal (8.3%, 4.6 g). FTIR (cm^{-1}): 3441 (br), 3083 (w), 3029 (w), 2919 (w), 2706 (w), 1604 (s), 1511 (vs), 1474 (s), 1350 (m), 1291 (s), 1240 (vs), 1173 (vs), 1108 (w), 1021 (m), 967 (m), 921 (m), 801 (vs), 742 (m). 1H NMR ($CDCl_3$, 400 MHz): δ.86 (s, 8H), 8.13−8.11 (m, 4H), 8.11−8.09 (m, 4H), 7.32−7.30 (m, 4H), 7.30−7.28 (m, 4H), 6.30 (dt, 2H), 6.24 (dd, 2H), 5.64 (q, 2H), 5.60 (q, 2H), 5.46 (q, 2H), 5.43 (q, 2H), 4.84 (t, 4H), 4.83 (t, 4H), −2.75 (s, 2H). ESI-MS (M+H) (m/z): 839.4, calcd for $C_{56}H_{47}N_4O_4$ (m/z), 838.4, Anal. Calcd for $C_{56}H_{46}N_4O_4$.

Preparation of PTCF/U-bent POF Probe. To fabricate the fiber probe, we utilized a multimode POF with core diameters of 980 μm and cladding diameters of 20 μm. The fiber has a core refractive index of 1.489 and NA value of 0.5. About 3 cm of the jacket was removed from the central portion of the fiber. This straight portion was bent slowly until it became U-shaped in a hot water bath (65−70 °C). Additional care was taken to maintain an optimum temperature and bending force. U-bent section was then immersed into acetone for 5 s, followed immersed into isopropanol for 10 s to ensure that a complete removal of the cladding. When finally washed with deionized water, the U-bent POF probe was drying in air circulation oven.

The principle of the U-bent fused-silica fiber probe has been explained by Khijwania,[45] and we can consider the results as a similar analysis for U-bent POF probe. As shown in Figure 1, when a light beam propagating through a transparent medium of high index of refraction encounters an interface with a medium of a lower index of refraction, it undergoes total internal reflection (TIR) for incidence angles greater than the "critical angle" of θ_c, which is given by

$$\theta_c = \sin^{-1}(n_2/n_1) \quad (1)$$

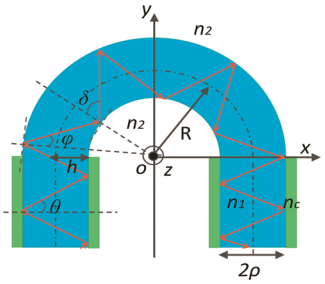

Figure 1. Schematic diagram of U-bent POF. (R, the bending radius; ρ, the fiber core radius; h, the ray's entrance height; n_2, the refractive indices of the surrounding; n_1, the refractive indices of the fiber core; θ, the incidence angle; φ and δ, the incidence angle at the outer and inner surface with respect to the normal to the interface, respectively).

where n_2 and n_1 are the refractive indices of the surrounding (1.407) and the fiber core (1.489), respectively. Despite the fact that the incident light beam totally internally reflects at the interface, the electromagnetic field called the "evanescent wave" still penetrates a small distance into the liquid medium and propagates parallel to the surface in the plane of incidence. The evanescent wave is capable of exciting fluorescent molecules that might be present near the interface. The evanescent electric field intensity decays exponentially with perpendicular distance z from the interface. This penetration depth (d) can be calculated from the incident wavelength (λ) (the free space wavelength of the light launched into the fiber) and the incidence angle (θ) (the ray with respect to the normal at the core−clad interface in the fiber) using

$$d = \frac{\lambda}{2\pi n_1(\cos^2\theta_c - \cos^2\theta^{1/2})} \quad (2)$$

If all the incident rays are launched at the input end of the straight fiber, the incidence angle (θ) varies from ~75° to 90°.[45] Because the experiment is performed only with the probe having uniform core diameter in entire U-shape region, Khijwania's method[45] can be used to solve this problem: θ changes from φ_1 to φ_2 at the outer surface, and from δ_1 to δ_2 at the inner surface with respect to the normal to the interface, where

$$\varphi_1 = \sin^{-1}\left[\left(\frac{R+h}{R+2\rho}\right)\frac{n_c}{n_1}\right] \quad (3)$$

and,

$$\varphi_2 = \sin^{-1}\left[\left(\frac{R+h}{R+2\rho}\right)\right] \quad (4)$$

whereas,

$$\delta_1 = \sin^{-1}\left[\left(\frac{R+h}{R}\right)\frac{n_c}{n_1}\right] \quad (5)$$

with $\delta_2 = 90°$. In eqs 2−4, n_c is refractive index of cladding, R is the bending radius, ρ is the fiber core radius, h is the ray's entrance height. Therefore, for a certain bending radius, θ becomes a function of h and ρ, and hence d can be calculated by using meridional ray approximations at the outer as well as at the inner surface of the fiber in the U-bent section for different core diameters and different ray's entrance height (h). h varies from 0 to 2ρ. Calculated value correspond to the skewness angle is equal to 90°. The bending radius used in our study is 5 mm and the incident wavelength (λ) for reaction is 365 nm. We can calculate φ_1 varies from 52.0 to 70.4°, φ_2 varies from 56.7° to 90°, meanwhile δ_1 varies from 70.4° to 90° by using eqs 3 and 4. Because of the critical angle of θ_c in U-bent section is 71°, and thus the incidence angle (θ) varies from ~71° to 90° at the outer or inner surface, otherwise optical propagation would not meet the total internal reflection (TIR). Ultimately, according to eq 2, the penetration depth d varies with a minimum value of 120.1 nm, the minimum thickness value of PTCF.

Utilizing this strategy, a PTCF/U-bent POF probe could be obtained by "click" polymerization *in situ*, as shown in Figure 2a. A

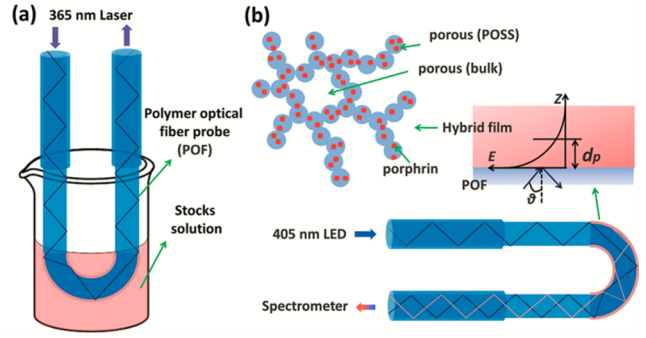

Figure 2. (a) Fabrication process and (b) schematic diagram of U-bent POF probe. A 365 nm laser is used for polymerization and 405 nm diode laser is selected for excitation of the porphyrin.

stock solution containing POSS-V8 (0.13 g, 0.2 mmol), 1, 6-hexanedimercaptan (75 uL, 0.5 mmol), allylporphyrin (0.3 mL × 10^{-3} M dye/THF solution) and UV photoinitiator DMPA (2 mg) in 0.7 mL THF was prepared and stirred in a dark place until all compounds were dissolved. A 365 nm laser (max. 35 mW/cm^2, adjustable), as actinic light source, was coupled to POF. The U-bent POF was placed in contact with the stock solution and UV light emerging from the fiber core induced polymerization in the U-bent section. The irradiation time was 10 s. After washing with isopropanol, the hybrid porous fluorescent layer was generated. Careful operation was required to ensure no damages caused by the shear force and complete coating on the uncladding surface, and thus optical loss of exciting light could be reduced in the U-bent section. Allylporphyrin in THF solution was further directly dropped to U-bent section as a contrast experiment.

Sensor Setup and Fluorescence Quenching Test. The setup is schematically shown in Figure S1 in the Supporting Information. The optical setup used for experiments consists of a blue LED (405 nm) and fiber optic spectrometer USB4000 (Ocean Optics, USA). The PTCF/U-bent POF probe can be temporarily fixed on a PMMA box (size: 65 mm × 45 mm × 18 mm, approximately 54 mL), with a gas-circulating system. First, the box without fiber probe was used to be saturated by TNT and DNT vapor. This method was performed according to the previous reports.[46−48] A sealed oblate (15 mL) beaker was filled with a small amount of solid explosive, and then set over 24 h to ensure saturation vapor pressure had been reached. Under this circumstance, concentrations of explosives in the box are 10 ppb for TNT, 180 ppb for DNT and 3 × 10^5 ppb for NB, respectively. Fluorescence quenching test was performed by inserting PTCF/U-bent POF probe into the PMMA box. Fluorescent emission from the other end of the fiber was evaluated immediately at room temperature. The fluorescence recovery experiment was conducted by washing with isopropanol and then drying in the air. In addition, the effect of organic volatile solvents (MeOH, CH_3CH_2OH, toluene, diethyl ether) to PTCF/U-bent POF probe was also tested. PTCF coated onto a hydrophobic quartz plate (treated by methyl trichlorosilane) was prepared by photopolymerization of diluted stock solution (1 mL in 29 mL of THF). The sensing test method of films (with thickness less than 500 nm) was the same to the previous reports.[46−48]

RESULTS AND DISCUSSION

Allylporphyrin monomer was prepared by "one pot" reaction of allyloxybenzaldehyde and pyrrole with propionic acid as solvent. The chemical structure was characterized by using ^{1}H NMR and mass spectra (see Figures S16−S19 in the

dx.doi.org/10.1021/am505950c | ACS Appl. Mater. Interfaces 2015, 7, 241−249

Supporting Information). As shown in Scheme 1, vinyl groups exist in POSS-V8 and porphyrin displayed similar reactivity

Scheme 1. Synthetic Route of Allylporphyrin and Preparation of PTCF

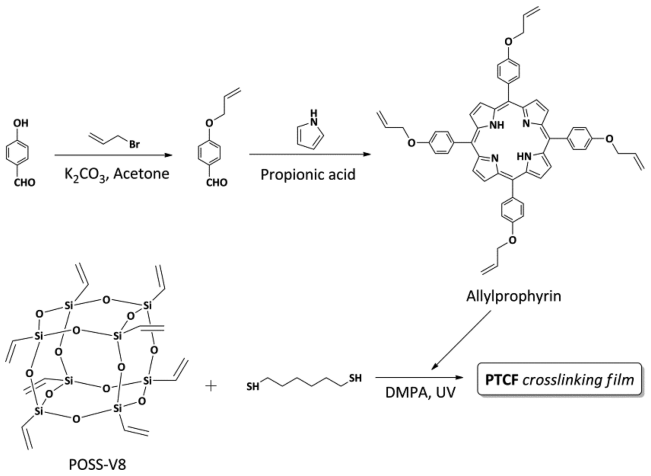

with thiol groups via thiol−ene "click" chemistry. Photoinduced thiol−ene polymerizations are known to react rapidly to form highly uniform polymer networks with narrow glass transitions and easily tailorable mechanical properties.[49,50] The step-growth mechanism of polymerization favors the formation of multiple low-molecular-weight species prior to gelation, resulting in high conversions at the gel point and largely homogeneous, three-dimension cross-linking film, PTCF. These characteristics present several significant advantages over classical radical chain-growth polymerizations involving acrylates and methacrylates that often suffer from low pregel conversion and form more heterogeneous networks.

Evanescent wave based sensitivity (absorbance or fluorescence) of fiber sensor probes can be increased by modifying the probe geometry including straight, U-bent, tapered tip, and biconical tapers.[51] We chose U-bent POF because of their sensitivity, compactness, ease in fabrication, and possibly higher compatibility with instrument configurations.[52] U-bent fiber probe has even been demonstrated to have a 10-fold improvement in absorbance sensitivity over straight probes.[53] Figure 2 illustrated the fabrication process of PTCF/U-bent POF probe *in situ* via "click" polymerization induced by 365 nm light existed in the evanescent wave at the bent region. This strategy can avoid both of physical damage of POF because of the solubility and causticity of bulk poly(methyl methacrylate) resin in organic solvents. On the other hand, the *in situ* method has been proved to be able to effectively modify the designed areas.[54] In the probe setup shown in Figure 2b, excitation (405 nm) is irradiated on one end of the fiber and the fluorescent emitted from the other end is collected using a fiber optic mini-spectrofluorimeter.

PTCF was characterized when isolated from a solution of PTCF/U-bent POF probe dissolved in acetone. It is found that overstoichiometric vinyl monomer could improve the hydrophobicity of PTCF (see Figure S2 in the Supporting Information), which can enhance the compatibility of PTCF with bulk poly(methyl methacrylate) resin.[40,55] FTIR spectroscopy (Figure 3a) of POSS-V8 and PTCF showed a very intense band at 1108 cm^{-1}, which is assigned to the Si−O−Si stretching vibration of POSS.[56] The existence of the vinyl

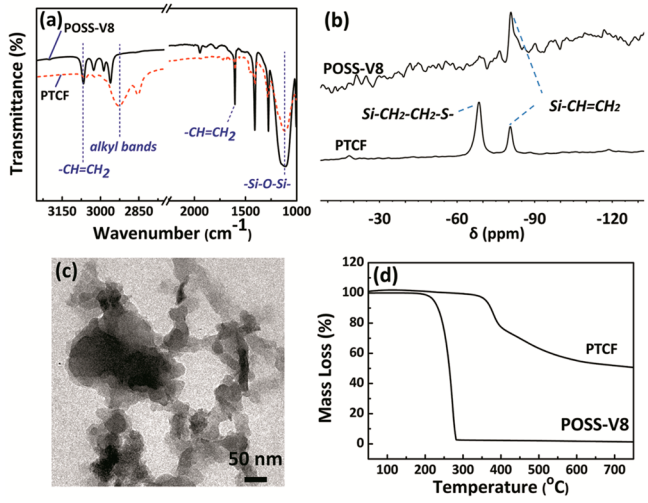

Figure 3. (a) FTIR spectra of POSS-V8 and PTCF. (b) ^{29}Si solid state NMR spectroscopy of POSS-V8 and PTCF. (c) TEM image of PTCF. (d) TG curves of POSS-V8 and PTCF.

groups is verified by the bands at 1604 cm^{-1} associated with the C=C stretching vibration, 3068 and 3029 cm^{-1} attributed to the C−H stretching vibration of vinyl groups.[56] The intensity of the vinyl bands of PTCF significantly decreases and new alkyl bands appears at 2900 cm^{-1}, indicating that "click" reaction has successfully proceeded. This result is confirmed by solid-state ^{29}Si NMR spectroscopy (Figure 3b), in which the shift of the neighboring silicon nuclei upon polymerization can be seen. POSS-V8 shows a broad resonance at δ = 78.9 ppm, corresponded to the T3 (CH_2=CH−Si$(OSi)_3$) type silicon.[57] PTCF shows two broad resonances at δ = 79.2 and 64.6 ppm, which can be assigned to T3 (CH_2=CH−Si$(OSi)_3$) and T3 (alkyl-Si$(OSi)_3$) type silicon signals.[57] The integration ratio between T3 (CH_2=CH−Si$(OSi)_3$) type silicon signals is approximately 1:2.3, indicating that the cross-linking degree of PTCF is ca. 69.7%.

Macroscopic morphologies of PTCF were observed by using TEM (Figure 3c). The product consists of irregularly shaped particles with a size of less than 50 nm, which appear to be formed by the initial cross-linking process between vinyl groups and thiol groups. Nitrogen adsorption experiment (see Figure S3 in the Supporting Information) further confirms the forming of porous structures with nano size. Nanoparticles could further react with each other, and thus bigger pores appear, as seen in Figure 3c. Compared with POSS-V8 precursor, PTCF displays high thermal stability (Figure 3d). In the case of POSS-V8, approximately 97.8% weight loss is observed at the temperature above 281.8 °C in N_2, which can be attributed to the thermal decomposition of −Si−O−Si− skeleton of POSS cage. However, PTCF displays higher thermal stability at the temperature below 350 °C in N_2 and approximately 50.0% weight residual rate. The phenomenon has been observed on other POSS-containing cross-linked materials.[57,58]

Absorptions of allylporphyrin in THF solution (Figure 4) can be attributed to $\pi-\pi^*$ electronic transitions: for the allylporphyrin and PTCF, the Soret band appears at 421 nm, while assorted Q bands are respectively displayed within 500−650 nm range, which are all identical with that reported before.[59] The shape of the absorption of PTCF is evidently no broadened to that of allylporphyrin. This result demonstrates that each porphyrin unit in PTCF is monodispersed without

dx.doi.org/10.1021/am505950c | ACS Appl. Mater. Interfaces 2015, 7, 241−249

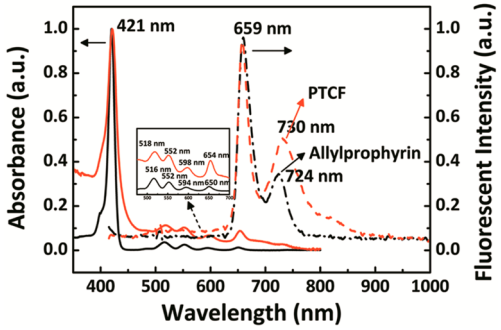

Figure 4. UV−vis absorbance and fluorescent spectra of allylporphyrin (in tetrahydrofuran solution) and PTCF.

aggregation interactions. In the fluorescence spectra (Figure 4) in solution, two major bands are both observed for allylporphyrin (659 and 724 nm) and PTCF (659 and 730 nm). PTCF can emit a bright red fluorescence but no fluorescence can be seen for allylporphyrin powder at the same conditions due to the complete fluorescence self-quenching. PTCF also shows a superior resistance to photobleaching than allylporphyrin powder (see Figure S4 in the Supporting Information).

The dip-coating technique works very well for producing thin films on supports such as silica glass and polished silicon wafers. However, the coating for optical fibers was proved to be difficult. A suitable dipping speed and concentration is crucial to wetting of the fiber surface and a smooth and relatively homogeneous film.[60] In our experiment, after *in situ* "click" chemistry, PTCF could fast cover on the side surface of U-bent POF. The smooth surface (SEM image in Figure 5a) of U-bent POF becomes porous (Figure 5b). SEM image also indicates that the thickness of PTCF is greater than 120 nm (Figure 5c), corresponding to the theoretical calculation results before.

The excited state of porphyrins can be quenched by an energy transfer to electron deficient explosive compounds upon collision with them, such as TNT, DNT, and NB.[61,62]

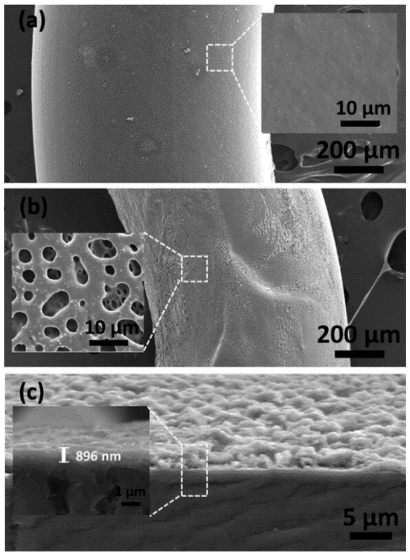

Figure 5. Scanning electron microscopy image of surface of (a) U-bent POF probe with directly dropped porphyrin molecule and (b) PTCF/U-bent POF probe. (c) Microtopography of the cross-section of PTCF/U-bent POF probe.

Fluorescence quenching is observed for the PTCF/U-bent POF probe upon exposure to TNT vapor. Figure 6a shows the

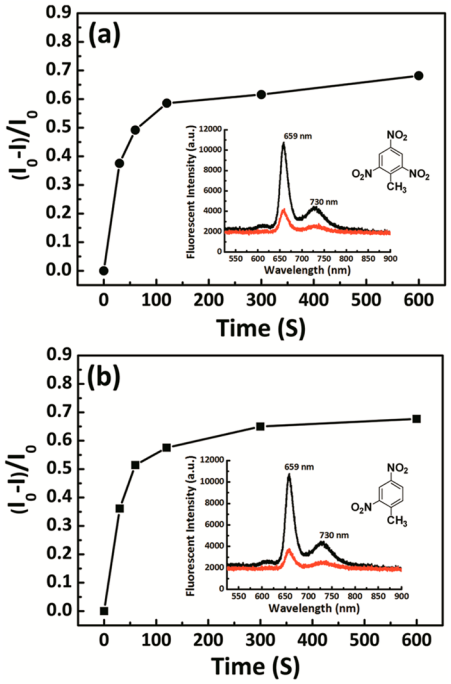

Figure 6. Quenching efficiencies $((I_0 - I)/I_0)$ of PTCF/U-bent POF probe with respect to time: (a) TNT and (b) DNT. The inset: fluorescence intensity curves of fiber probe exposed to (a) TNT and (b) DNT for 0 s (black curve) and 300 s (red curve), respectively.

quenching efficiencies $((I_0 - I)/I_0)$ of the PTCF/U-bent POF probe with respect to time. As shown in Figure 6a and Figure S5 in the Supporting Information, the fiber probe is found to have quenching efficiencies of 37.5% at 30 s and 61.6% in 300 s, respectively. This high quenching efficiency might derive mainly from high porosity of PTCF. Nanoporous of POSS and macropores of the bulk PTCF, as shown in Figure 3c and Figure 5b, c, enables faster diffusion of the explosive molecules. The fiber probe is found to have quenching efficiencies of 36.1% in 30 s and 65.0% in 300 s for DNT (Figure 6b and Figure S6 in the Supporting Information), and quenching efficiencies of 8.8% in 30 s and 21.1% in 300 s for NB (Figures S7 and S8 in the Supporting Information), respectively. Directly dropping the solution of allylporphyrin onto the surface can weaken quenching efficiency of U-bent POF probe (see Figures S9 and S10 in the Supporting Information). Fluorescent quenching efficiency of quartz plate coated with the PTCF is closed to that of the fiber probe, as shown Figure S11 in the Supporting Information.

Three different dithiol-teminated polyethylene glycols (SH-PEG-SH, Figure S12 in the Supporting Information) were synthesized in order to gain macroporous coatings with different pore diameters (see Figure S13 in the Supporting Information). Compared with 1,6-hexanedimercaptan with molecular length of 0.9263 nm (calculated by Chemoffice 3D), the straight SH-PEG-SH has a longer molecular length, for instance, 5.1062 nm for PEG600 (see Figure S12 in the Supporting Information). In principle, the size of pores is related with macromolecular length. However, the fluorescence quenching test through macroporous films coated onto a quartz plate showed a slow response behavior (see Figure S13 in the

dx.doi.org/10.1021/am505950c | ACS Appl. Mater. Interfaces 2015, 7, 241−249

Supporting Information). The flexibility of polymer chains might result in macromolecular coil, and forming compact layer to discourage diffusion of TNT vapor.

In Figure 6, quenching efficiency of PTCF/U-bent POF probe for TNT was approximately equal to the quenching efficiency for DNT in the first minute. After the second minute, quenching efficiency for TNT increases a little lower than that for DNT. Generally speaking, the binding constant of TNT to electron-rich porphyrin ring is higher than DNT because of its extra electron-withdrawing nitro group. But, unlike Tetrakis(4-carboxyphenyl)porphyrin (TCPP), the quenching constant (K_{sv}, obtained by Stern–Volmer plot: $I_0/I = 1 + K_{sv}[C]$) of allylporphyrin is 85.5 and 77.0 for TNT and DNT, respectively (Figure S14 and Table S1 in the Supporting Information). In fact, some porphyrins with electron-rich substituents at the periphery have a similar value of K_{sv} for TNT and DNT.[61] In addition, fluorescence quenching efficiency is also affected by the vapor pressure of explosives. So, similar fluorescence responses mainly come from the higher volatility of DNT than TNT.

In Figure 6a, the quenching efficiency $((I_0 - I)/I_0)$ of PTCF/U-bent POF probe for TNT initially shows a linear behavior, however, under longer exposure it displayed downward curvature. The downward curvature is likely to reflect a saturation phenomenon: TNT first permeates into nanopores with strong bonding ability (linear part of the plot), which is followed by much slower diffusion into bulk macropores with weak bonding ability. The two kinds of pore structures were demonstrated before,[63] and the permeation capacity is further analyzed by the modified Stern–Volmer equation, which is approximately described by eq 6[63]

$$\frac{I_0}{\Delta I} = \frac{1}{f_a} + \frac{1}{f_a K_a t} \quad (6)$$

where I_0 is the initial fluorescence intensity, $\Delta I = I_0 - I$ is the fluorescence intensity difference after exposure to explosive, f_a is the fraction of easy permeation capacity, K_a is the effective quenching constant and t is the exposure time. The modified Stern–Volmer plots obtained for PTCF/U-bent POF probe are shown in Figure 7. The dependence of $I_0/\Delta I$ on the reciprocal value of the exposure time is linear with slope equal to the value of $(f_a K_a)^{-1}$. The value f_a^{-1} can be obtained by extending the line to the ordinate. The corresponding results shows a linear function for diffusing of TNT into PTCF, as shown in Figure 7a, and, thus, the fraction of easy permeation capacity f_a was 0.70. Although f_a was less than that of molecularly imprinted CPs reported in literature which were prepared by sophisticated template-removal procedure,[63] PTCF/U-bent POF probe can be considered to be an excellent candidate for rapid detecting nitroaromatic vapor even without any complex design. In Figure 7b, the relationship of $I_0/\Delta I \sim t^{-1}$ showed distinct nonlinearly for U-bent probe with the dropping method (fluorescence quenching curve in Figures S9 and S10 in the Supporting Information). That could arise from the complicated diffusion modes into bulk polymer resin (Figure 7c, compared to diffusion into PTCF shown in Figure 7d), for instances, the combined effect caused by diffusion and solubility processes.

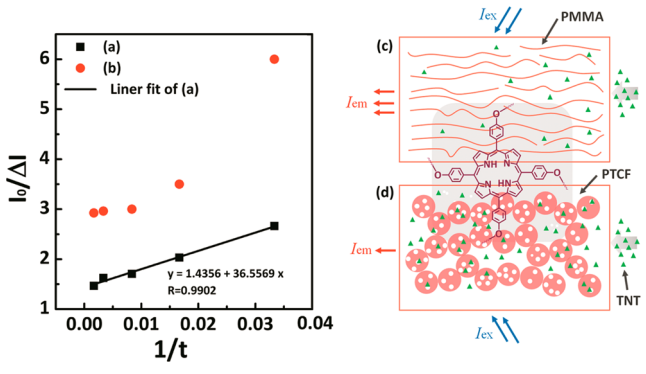

Figure 7. Modified Stern–Volmer plots of U-bent POF probe: (a) PTCF/U-bent POF probe with a linear function and (b) U-bent probe with the dropping method. Schematic diagram of TNT vapor diffusing into PMMA resin (c) and PTCF (d).

As high binding strength of TNT to porphyrin ring, the fluorescence recovery is very slow in room condition. Under this circumstance, the reversibility of the sensing process was examined with TNT vapor as a representative nitroaromatic compounds (Figure 8). After exposure to TNT vapor, the fiber probe was ultrasonic washing by isopropanol, followed air-dried. The recovered probe shows approximately quenching efficiency when re-exposed to the TNT vapor. Efficient quenching and recovery are necessary for practical utilities, and the result above implys that a good reversibility and a highly fluorescence stability for the fiber probe against photobleaching could be achieved. However, for the dropping method porphyrin molecule could effusion from bulk poly-(methyl methacrylate) resin by ultrasonic washing with isopropanol. As seen in Figure 8b, fluorescent intensity of signal accepted from the fiber tip decayed along with the increase of cycle number. In addition, PTCF/U-bent POF probe displays a character that fluorescent signal could never be changed by the action of other organic volatile solvents, as shown in Figure S15 in the Supporting Information.

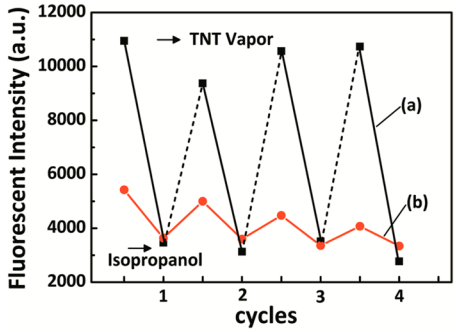

Figure 8. Fluorescence quenching-recovery cycles test after the fiber probe exposing to TNT for 300 s, and the ultrasonic washing with isopropanol as solvent: (a) PTCF/U-bent fiber probe and (b) drop method.

In all cases, as we known, interaction between the individual vapor molecule and the surface of the sensing element can affect both of the sensitivity and the reaction time. Sensor materials with high K_{sv} and high specific accessible surface areas are beneficial, which is why fluorescent porous films are particularly suitable. As shown in Table S2 in the Supporting Information, compared to conventional optical fiber sensor systems, PTCF coated onto U-bent POF may offer some further advantages: the option to finely disperse active species (dyes, nanoparticles, etc.), accessible precursor materials, facile

preparation process, and high stability in terms of their specific gas diffusion phenomena within the pores.

CONCLUSIONS

In summary, the surface functionalization of poly(methyl methacrylate) optical fiber with fluorescent porous thin film is achieved *in situ* via "click" chemistry. Polyhedral oligomeric vinylsilsesquioxane (POSS-V8) containing multienes, porphyrin with four allyl groups and 1, 6-Hexanedimercaptan containing two thiol groups are used as precursors of the thiol−ene "click" reaction for the film. Upon irradiation of evanescent UV light transmitting within the fiber immersed in the precursors a cross-linked film is formed on the side surface of the fiber under ambient condition. In PTCF/U-bent POF probe made by this method, porphyrin is chemically stable in POSS-containing film as fluorescence response material. Aggregation-induced fluorescence self-quenching of porphyrin is deleted by the "fastened" network. Fluorescent signals of PTCF/U-bent POF probe exhibit high fluorescence quenching toward trace TNT (10 ppb, 37.5% for 30 s), DNT (180 ppb, 36.1% for 30s) and NB (3 × 105 ppb, 8.8% for 30 s). Comparison with the method by directly dropping the solution of porphyrin on the side surface POF, "click" reaction not only affords the path to steady disperse dyes, but also constructs a porous film for more rapid response toward TNT and DNT vapor. This kind of easily prepared fluorescent porous film is promising candidates for extensive application of polymer optical fiber probe.

ASSOCIATED CONTENT

Supporting Information

Schematic diagram of sensor setup and fluorescence quenching test. Transmittance and contact angle of PTCF (Cross-linked on the surface of quartz glass). Pore size distribution curve of PTCF. Photostability of PTCF and porphyrin powder. Fluorescence quenching curve of PTCF/U-bent POF probe (analyte = TNT, DNT and NB). The quenching efficiencies of PTCF/U-bent POF probe (analyte = NB). Fluorescence quenching curve and the quenching efficiencies of PTCF/U-bent POF probe by dropping method (analyte = TNT). Fluorescence quenching curve and the quenching efficiencies of the quartz plate coated with the fluorescent porous film. Molecular length of dithiol compounds calculated by Chemoffice 3D. SEM image of the fluorescent porous film, and corresponding fluorescence quenching curve of the quartz plate coated with the PTCF. Stern−Volmer plot, quenching constant and the linear relation of allylporphyrin and TCPP. Interference experiment of PTCF/U-bent POF probe. Comparison of the preparation process and sensor properties of representative optical fiber sensor. Additional molecular and structural characterization data. This material is available free of charge via the Internet at http://pubs.acs.org.

AUTHOR INFORMATION

Corresponding Author

*E-mail: zqjm@ustc.edu.cn. Phone: 86-550-63607874. Fax: 86-550-63607874.

Notes

The authors declare no competing financial interest.

ACKNOWLEDGMENTS

This work is supported by National Natural Science Foundation of China (21074123, 91027024, 51173176, and 51273186).

REFERENCES

(1) Toal, S. J.; Trogler, W. C. Polymer Sensors for Nitroaromatic Explosives Detection. *J. Mater. Chem.* **2006**, *16*, 2871−2883.
(2) Kartha, K. K.; Babu, S. S.; Srinivasan, S.; Ajayaghosh, A. Attogram Sensing of Trinitrotoluene with a Self-Assembled Molecular Gelator. *J. Am. Chem. Soc.* **2012**, *134*, 4834−4841.
(3) Pushkarsky, M. B.; Dunayevskiy, I. G.; Prasanna, M.; Tsekoun, A. G.; Go, R.; Patel, C. K. N. High-Sensitivity Detection of TNT. *Proc. Natl. Acad. Sci. U. S. A.* **2006**, *103*, 19630−19634.
(4) Takáts, Z.; Cotte-Rodriguez, I.; Talaty, N.; Chen, H.; Cooks, R. G. Direct, Trace Level Detection of Explosives on Ambient Surfaces by Desorption Electrospray Ionization Mass Spectrometry. *Chem. Commun.* **2005**, *15*, 1950−1952.
(5) Fayazi, M.; Ghanei-Motlagh, M.; Taher, M. A. Combination of Carbon Nanotube Reinforced Hollow Fiber Membrane Microextraction with Gas Chromatography-Mass Spectrometry for Extraction and Determination of Some Nitroaromatic Explosives in Environmental Water. *Anal. Methods.* **2013**, *5*, 1474−1480.
(6) Piorek, B. D.; Lee, S. J.; Moskovits, M.; Meinhart, C. D. Free-Surface Microfluidics/Surface-Enhanced Raman Spectroscopy for Real-Time Trace Vapor Detection of Explosives. *Anal. Chem.* **2012**, *84*, 9700−9705.
(7) Tam, M.; Hill, H. H. Secondary Electrospray Ionization-Ion Mobility Spectrometry for Explosive Vapor Detection. *Anal. Chem.* **2004**, *76*, 2741−2747.
(8) Beyazkilic, P.; Yildirim, A.; Bayindir, M. Formation of Pyrene Excimers in Mesoporous Ormosil Thin Films for Visual Detection of Nitro-Explosives. *ACS Appl. Mater. Interfaces* **2014**, *6*, 4997−5004.
(9) Yildirim, A.; Acar, H.; Erkal, T. S.; Bayindir, M.; Guler, M. O. Template-Directed Synthesis of Silica Nanotubes for Explosive Detection. *ACS Appl. Mater. Interfaces* **2011**, *3*, 4159−4164.
(10) Nie, H.; Zhao, Y.; Zhang, M.; Ma, Y.; Baumgarten, M.; Müllen, K. Detection of TNT Explosives with a New Fluorescent Conjugated Polycarbazole Polymer. *Chem. Commun.* **2011**, *47*, 1234−1236.
(11) Yang, J.-S.; Swager, T. M. Porous Shape Persistent Fluorescent Polymer Films: an Approach to TNT Sensory Materials. *J. Am. Chem. Soc.* **1998**, *120*, 5321−5322.
(12) He, G.; Yan, N.; Yang, J.; Wang, H.; Ding, L.; Yin, S.; Fang, Y. Pyrene-Containing Conjugated Polymer-based Fluorescent Films for Highly Sensitive and Selective Sensing of TNT in Aqueous Medium. *Macromolecules* **2011**, *44*, 4759−4766.
(13) Xu, S.; Lu, H.; Li, J.; Song, X.; Wang, A.; Chen, L.; Han, S. Dummy Molecularly Imprinted Polymers-Capped CdTe Quantum Dots for the Fluorescent Sensing of 2, 4, 6-Trinitrotoluene. *ACS Appl. Mater. Interfaces* **2013**, *5*, 8146−8154.
(14) Farooq, A.; Al-Jowder, R.; Narayanaswamy, R.; Azzawi, M.; Roche, P. J.; Whitehead, D. E. Gas Detection using Quenching Fluorescence of Dye-Immobilised Silica Nanoparticles. *Sens. Actuators, B* **2013**, *183*, 230−238.
(15) Pulido, C.; Esteban, Ó. Tapered Polymer Optical Fiber Oxygen Sensor Based on Fluorescence-Quenching of an Embedded Fluorophore. *Sens. Actuators, B* **2013**, *184*, 64−69.
(16) Luo, Y.; Zhou, J.; Yan, Q.; Su, W.; Li, Z.; Zhang, Q.; Huang, J.; Wang, K. Optical Manipulable Polymer Optical Fiber Bragg Gratings with Azopolymer as Core Material. *Appl. Phys. Lett.* **2007**, *91*, 071110.
(17) Mizuno, Y.; Hayashi, N.; Tanaka, H.; Nakamura, K.; Todoroki, S.-i. Observation of Polymer Optical Fiber Fuse. *Appl. Phys. Lett.* **2014**, *104*, 043302.
(18) Liang, H.; Zhang, Q.; Zheng, Z.; Ming, H.; Li, Z.; Xu, J.; Chen, B.; Zhao, H. Optical Amplification of Eu $(DBM)_3$ Phen-doped Polymer Optical Fiber. *Opt. Lett.* **2004**, *29*, 477−479.

(19) Luo, Y.; Zhang, Q.; Liu, H.; Peng, G.-D. Gratings Fabrication in Benzildimethylketal Doped Photosensitive Polymer Optical Fibers using 355 nm Nanosecond Pulsed Laser. *Opt. Lett.* **2010**, *35*, 751−753.
(20) Hu, Z.; Miao, B.; Wang, T.; Fu, Q.; Zhang, D.; Ming, H.; Zhang, Q. Disordered Microstructure Polymer Optical Fiber for Stabilized Coherent Random Fiber Laser. *Opt. Lett.* **2013**, *38*, 4644−4647.
(21) Ho, M.-L.; Wang, J.-C.; Wang, T.-Y.; Lin, C.-Y.; Zhu, J. F.; Chen, Y.-A.; Chen, T.-C. The Construction of Glucose Biosensor Based on Crystalline Iridium (III)-Containing Coordination Polymers with Fiber-Optic Detection. *Sens. Actuators, B* **2014**, *190*, 479−485.
(22) MacCraith, B. D.; McDonagh, C. M.; O'Keeffe, G.; Keyes, E. T.; Vos, J. G.; O'Kelly, B.; McGilp, J. F. Fibre Optic Oxygen Sensor Based on Fluorescence Quenching of Evanescent-Wave Excited Ruthenium Complexes in Sol−Gel Derived Porous Coatings. *Analyst* **1993**, *118*, 385−388.
(23) Tang, X.; Provenzano, J.; Xu, Z.; Dong, J.; Duan, H.; Xiao, H. Acidic ZSM-5 Zeolite-Coated Long Period Fiber Gating for Optical Sensing of Ammonia. *J. Mater. Chem.* **2011**, *21*, 181−186.
(24) Zhao, Q.; Yin, M.; Zhang, A. P.; Prescher, S.; Antonietti, M.; Yuan, J. Hierarchically Structured Nanoporous Poly (Ionic Liquid) Membranes: Facile Preparation and Application in Fiber-Optic pH Sensing. *J. Am. Chem. Soc.* **2013**, *135*, 5549−5552.
(25) Zhang, Y.; Xue, L.; Wang, T.; Yang, L.; Zhu, B.; Zhang, Q. High Performance Temperature Sensing of Single Mode-Multimode-Single Mode Fiber with Thermo-Optic Polymer as Cladding Of Multimode Fiber Segment. *IEEE Sens. J.* **2014**, *14*, 1143−1147.
(26) Orghici, R.; Willer, U.; Gierszewska, M.; Waldvogel, S.; Schade, W. Fiber Optic Evanescent Field Sensor for Detection of Explosives and CO_2 Dissolved in Water. *Appl. Phys. B: Lasers Opt.* **2008**, *90*, 355−360.
(27) Van Bergen, S. K.; Bakaltcheva, I. B.; Lundgren, J. S.; Shriver-Lake, L. C. On-Site Detection of Explosives in Groundwater with a Fiber Optic Biosensor. *Environ. Sci. Technol.* **2000**, *34*, 704−708.
(28) Cennamo, N.; D'Agostino, G.; Galatus, R.; Bibbo, L.; Pesavento, M.; Zeni, L. Sensors Based on Surface Plasmon Resonance in a Plastic Optical Fiber for The Detection of Trinitrotoluene. *Sens. Actuators, B* **2013**, *188*, 221−226.
(29) El Hamzaoui, H.; Bigot, L.; Bouwmans, G.; Razdobreev, I.; Bouazaoui, M.; Capoen, B. From Molecular Precursors in Solution to Microstructured Optical Fiber: A Sol-Gel Polymeric Route. *Opt. Mater. Express.* **2011**, *1*, 234−242.
(30) Chu, C.-S.; Lo, Y.-L. Optical Fiber Dissolved Oxygen Sensor Based on Pt (II) Complex and Core-Shell Silica Nanoparticles Incorporated with Sol−Gel Matrix. *Sens. Actuators, B* **2010**, *151*, 83−89.
(31) Yeh, T.-S.; Chu, C.-S.; Lo, Y.-L. Highly Sensitive Optical Fiber Oxygen Sensor using Pt (II) Complex Embedded in Sol−Gel Matrices. *Sens. Actuators, B* **2006**, *119*, 701−707.
(32) Fierke, M. A.; Olson, E. J.; Bühlmann, P.; Stein, A. Receptor-Based Detection of 2,4-Dinitrotoluene using Modified Three-Dimensionally Ordered Macroporous Carbon Electrodes. *ACS Appl. Mater. Interfaces* **2012**, *4*, 4731−4739.
(33) Xu, S.; Sun, F.; Gu, F.; Zuo, Y.; Zhang, L.; Fan, C.; Yang, S.; Li, W. Photochemistry-Based Method for the Fabrication of SnO_2 Monolayer Ordered Porous Films with Size-Tunable Surface Pores for Direct Application in Resistive-Type Gas Sensor. *ACS Appl. Mater. Interfaces* **2014**, *6*, 1251−1257.
(34) Lee, D.; Kim, S.; Jeon, S.; Thundat, T. Direct Detection and Speciation of Trace Explosives using a Nanoporous Multi-Functional Microcantilever. *Anal. Chem.* **2014**, *86*, 5077−5082.
(35) Vu, A.; Phillips, J.; Bühlmann, P.; Stein, A. Quenching Performance of Surfactant-Containing and Surfactant-Free Fluorophore-Doped Mesoporous Silica Films for Nitroaromatic Compound Detection. *Chem. Mater.* **2013**, *25*, 711−722.
(36) Alves, F.; Scholder, P.; Nischang, I. Conceptual Design of Large Surface Area Porous Polymeric Hybrid Media Based on Polyhedral Oligomeric Silsesquioxane Precursors: Preparation, Tailoring of Porous Properties, and Internal Surface Functionalization. *ACS Appl. Mater. Interfaces* **2013**, *5*, 2517−2526.
(37) Nischang, I.; Brüggemann, O.; Teasdale, I. Facile, Single-Step Preparation of Versatile, High-Surface-Area, Hierarchically Structured Hybrid Materials. *Angew. Chem., Int. Ed.* **2011**, *50*, 4592−4596.
(38) Kiba, S.; Okawauchi, Y.; Yanagihara, T.; Murakami, M.; Shimizu, T.; Yamauchi, Y. Mesoporous Silica/Polymer Composites utilizing Intelligent Caps onto Mesopore Walls toward Practical Low-Dielectric Materials. *Chem.—Asian J.* **2009**, *4*, 1798−1801.
(39) Milliman, H. W.; Boris, D.; Schiraldi, D. A. Experimental Determination of Hansen Solubility Parameters for Select POSS and Polymer Compounds as a Guide to POSS−Polymer Interaction Potentials. *Macromolecules* **2012**, *45*, 1931−1936.
(40) Tuteja, A.; Choi, W.; Ma, M.; Mabry, J. M.; Mazzella, S. A.; Rutledge, G. C.; McKinley, G. H.; Cohen, R. E. Designing Superoleophobic Surfaces. *Science* **2007**, *318*, 1618−1622.
(41) Chatterjee, S.; Ramakrishnan, S. Defect-Free Hyperbranched Polydithioacetal via Melt Polymerization. *ACS Macro Lett.* **2012**, *1*, 593−598.
(42) Yang, T.; Long, H.; Malkoch, M.; Kristofer, E.; Berglund, L.; Hult, A. Characterization of Well-Defined Poly (Ethylene Glycol) Hydrogels Prepared by Thiol-Ene Chemistry. *J. Polym. Sci., Part A: Polym. Chem.* **2011**, *49*, 4044−4054.
(43) Jeong, E. Y.; Burri, A.; Lee, S. Y.; Park, S. E. Synthesis and Catalytic Behavior of Tetrakis (4-Carboxyphenyl) Porphyrin-Periodic Mesoporous Organosilica. *J. Mater. Chem.* **2010**, *20*, 10869−10875.
(44) Gaspar, B.; Carreira, E. M. Mild Cobalt-Catalyzed Hydrocyanation of Olefins with Tosyl Cyanide. *Angew. Chem., Int. Ed.* **2007**, *46*, 4519−4522.
(45) Khijwania, S. K.; Srinivasan, K. L.; Singh, J. P. An Evanescent-Wave Optical Fiber Relative Humidity Sensor with Enhanced Sensitivity. *Sens. Actuators, B* **2005**, *104*, 217−222.
(46) Yildirim, A.; Budunoglu, H.; Deniz, H.; Guler, M. O.; Bayindir, M. Template-Free Synthesis of Organically Modified Silica Mesoporous Thin Films for TNT Sensing. *ACS Appl. Mater. Interfaces* **2010**, *2*, 2892−2897.
(47) Tao, S.; Yin, J.; Li, G. High-Performance TNT Chemosensory Materials Based on Nanocomposites with Bimodal Porous Structures. *J. Mater. Chem.* **2008**, *18*, 4872−4878.
(48) Lv, Y.-Y.; Xu, W.; Lin, F.-W.; Wu, J.; Xu, Z.-K. Electrospun Nanofibers of Porphyrinated Polyimide for the Ultra-Sensitive Detection of Trace TNT. *Sens. Actuators, B* **2013**, *184*, 205−211.
(49) Sparks, B. J.; Hoff, E. F.; Xiong, L.; Goetz, J. T.; Patton, D. L. Superhydrophobic Hybrid Inorganic−Organic Thiol-ene Surfaces Fabricated via Spray-Deposition and Photopolymerization. *ACS Appl. Mater. Interfaces* **2013**, *5*, 1811−1817.
(50) Northrop, B. H.; Coffey, R. N. Thiol−Ene Click Chemistry: Computational and Kinetic Analysis of the Influence of Alkene Functionality. *J. Am. Chem. Soc.* **2012**, *134*, 13804−13817.
(51) Leung, A.; Shankar, P. M.; Mutharasan, R. A Review of Fiber-Optic Biosensors. *Sens. Actuators, B* **2007**, *125*, 688−703.
(52) Sai, V.; Kundu, T.; Mukherji, S. Novel U-Bent Fiber Optic Probe for Localized Surface Plasmon Resonance Based Biosensor. *Biosens. Bioelectron.* **2009**, *24*, 2804−2809.
(53) Gupta, B.; Dodeja, H.; Tomar, A. Fibre-Optic Evanescent Field Absorption Sensor Based on a U-Shaped Probe. *Opt. Quantum Electron.* **1996**, *28*, 1629−1639.
(54) Ton, X. A.; Tse Sum Bui, B.; Resmini, M.; Bonomi, P.; Dika, I.; Soppera, O.; Haupt, K. A Versatile Fiber-Optic Fluorescence Sensor Based on Molecularly Imprinted Microstructures Polymerized *in situ*. *Angew. Chem., Int. Ed.* **2013**, *52*, 8317−8321.
(55) Xue, Y.; Wang, H.; Yu, D.; Feng, L.; Dai, L.; Wang, X.; Lin, T. Superhydrophobic Electrospun POSS-PMMA Copolymer Fibres with Highly Ordered Nanofibrillar and Surface Structures. *Chem. Commun.* **2009**, *42*, 6418−6420.
(56) Monticelli, O.; Fina, A.; Cozza, E. S.; Prato, M.; Bruzzo, V. POSS Vapor Phase Grafting: A Novel Method to Modify Polymer Films. *J. Mater. Chem.* **2011**, *21*, 18049−18054.
(57) Yan, Z.; Xu, H.; Guang, S.; Zhao, X.; Fan, W.; Liu, X. Y. A Convenient Organic-Inorganic Hybrid Approach Toward Highly

Stable Squaraine Dyes with Reduced H-Aggregation. *Adv. Funct. Mater.* **2012**, *22*, 345−352.
(58) Chen, Q.; Xu, R.; Zhang, J.; Yu, D. Polyhedral Oligomeric Silsesquioxane (POSS) Nanoscale Reinforcement of Thermosetting Resin from Benzoxazine and Bisoxazoline. *Macromol. Rapid Commun.* **2005**, *26*, 1878−1882.
(59) Quiroz-Segoviano, R. I.; Serratos, I. N.; Rojas-González, F.; Tello-Solís, S. R.; Sosa-Fonseca, R.; Medina-Juárez, O.; Menchaca-Campos, C.; García-Sánchez, M. A. On Tuning The Fluorescence Emission of Porphyrin Free Bases Bonded to the Pore Walls of Organo-Modified Silica. *Molecules* **2014**, *19*, 2261−2285.
(60) Wirnsberger, G.; Stucky, G. D. Microring Lasing from Dye-Doped Silica/Block Copolymer Nanocomposites. *Chem. Mater.* **2000**, *12*, 2525−2527.
(61) Rana, A.; Panda, P. K. Fluorescent Turn-Off Based Sensing of Nitrated Explosives using Porphyrins and Their Zn (II)-Derivatives. *RSC Adv.* **2012**, *2*, 12164−12168.
(62) Tao, S.; Li, G. Porphyrin-Doped Mesoporous Silica Films for Rapid TNT Detection. *Colloid Polym. Sci.* **2007**, *285*, 721−728.
(63) Li, J.; Kendig, C. E.; Nesterov, E. E. Chemosensory Performance of Molecularly Imprinted Fluorescent Conjugated Polymer Materials. *J. Am. Chem. Soc.* **2007**, *129*, 15911−15918.